

Quantum diffusion with disorder, noise and interaction

C D'Errico^{1,5}, M Moratti¹, E Lucioni¹, L Tanzi¹, B Deissler^{1,2},
M Inguscio^{1,3}, G Modugno¹, M B Plenio⁴ and F Caruso^{1,3,4,5}

¹ LENS and Dipartimento di Fisica e Astronomia, Università di Firenze,
and INO-CNR, I-50019 Sesto Fiorentino, Italy

² Institut für Quantenmaterie, Universität Ulm, Albert-Einstein-Allee 45,
D-89069 Ulm, Germany

³ QSTAR, Largo Enrico Fermi 2, I-50125 Firenze, Italy

⁴ Institut für Theoretische Physik, Universität Ulm, Albert-Einstein-Allee 11,
D-89069 Ulm, Germany

E-mail: derrico@lens.unifi.it and filippo.caruso@lens.unifi.it

New Journal of Physics **15** (2013) 045007 (18pp)

Received 27 November 2012

Published 12 April 2013

Online at <http://www.njp.org/>

doi:10.1088/1367-2630/15/4/045007

Abstract. Disorder, noise and interaction play a crucial role in the transport properties of real systems, but they are typically hard to control and study, both theoretically and experimentally, especially in the quantum case. Here, we explore a paradigmatic problem, the diffusion of a wavepacket, by employing ultra-cold atoms in a quasi-periodic lattice with controlled noise and tunable interaction. The presence of quasi-disorder leads to Anderson localization, while both interaction and noise tend to suppress localization and restore transport, although with completely different mechanisms. When only noise or interaction is present, we observe a diffusion dynamics that can be explained by existing microscopic models. When noise and interaction are combined, we observe instead a complex anomalous diffusion. By combining experimental measurements with numerical simulations, we show that such anomalous behavior can be modeled with a generalized diffusion equation in which the noise- and interaction-induced diffusions enter in an additive manner. Our study reveals also a more complex interplay between the two diffusion mechanisms in the regimes of strong interaction or narrowband noise.

⁵ Authors to whom any correspondence should be addressed.



Content from this work may be used under the terms of the [Creative Commons Attribution 3.0 licence](http://creativecommons.org/licenses/by/3.0/). Any further distribution of this work must maintain attribution to the author(s) and the title of the work, journal citation and DOI.

Contents

1. Introduction	2
2. Experimental setup	3
2.1. Dynamics in a quasi-periodic lattice	3
3. Results	4
3.1. Observation of anomalous diffusion induced by noise and interaction	4
3.2. Noise-induced normal diffusion	5
3.3. Interaction-induced subdiffusion	7
3.4. The generalized diffusion model	7
4. Regimes of noise–interaction interplay	9
5. Summary	12
6. Conclusions and outlook	12
Acknowledgments	13
Appendix A. Experimental methods	13
Appendix B. Theoretical methods	15
References	17

1. Introduction

Disorder, noise and interaction are known to play a fundamental role in the dynamics of quantum systems, but a detailed understanding of their combined action is still lacking. The interest in this general problem is found in fields ranging from electronic systems [1], spin glasses [2] and nanoscale quantum Brownian motors [3], to quantum communication [4, 5] and the physics of biological complexes [6–10]. Despite its importance, there is to date only very limited theoretical understanding of the interplay among disorder, noise and interaction. Moreover, these ingredients are hard to control in experiments with natural or artificial systems; one exception is quantum optical schemes [11–14], where nonlinearities are, however, weak and do not allow one to investigate in depth the many-body effects.

The prototypical dynamical problem for disordered quantum systems is the evolution of an initially localized wavepacket [15]. To our knowledge this problem has never been studied earlier, neither theoretically nor experimentally, under the combined effect of noise and interaction. It is well known that in one spatial dimension a linear wavepacket is localized in a finite region of space by the Anderson localization mechanism. Noise is instead known to break the coherence that is necessary for achieving localization, giving rise to a diffusive expansion of the wavepacket, as predicted by several theoretical approaches [16–20] and also observed in experiments with atoms and photons [21–25]. Finally, also a weak interaction can inhibit the Anderson localization, through the coherent coupling of single-particle localized states [26–36], giving rise to a subdiffusion, i.e. a time-dependent diffusion coefficient, that has recently been observed in experiments with ultra-cold atoms [37]. A stronger interaction, in systems with limited kinetic energy such as lattices, can instead lead to other localization phenomena, such as self-trapping [38] or the Mott insulator [39]. In this regime, the presence of disorder can give rise to new quantum phases [40, 41]. However, while both microscopic theories and macroscopic models exist for noisy or many-body disordered systems, no such theory has been developed on the evolution of a wavepacket in disorder with the simultaneous

presence of noise and interaction effects. Even an intuitive understanding of the problem is prevented by the difficulty in combining the incoherent dynamics generated by noise with the coherent coupling due to interaction.

In this work, we employ an ultra-cold Bose–Einstein condensate in a quasi-periodic optical lattice (mimicking true disorder) to investigate the general features of the expansion of a wavepacket subjected to controlled broadband noise and weak repulsive or attractive interaction. In general, we find that the combination of noise and interaction gives rise to a faster, anomalous diffusion of the wavepacket, with a time exponent that depends in a complex manner on the system parameters. Our extensive exploration, supported by numerical simulations, indicates that such dynamics can be modeled quite accurately over a wide range of parameters by a generalized diffusion equation in which the two diffusion terms due to noise and interaction simply add up. This surprisingly simple result seems to persist also in regimes where perturbative modeling of the individual diffusion mechanisms breaks down. For particularly strong interaction strengths or narrowband noise, we find instead a more complex interplay of noise and interaction in the expansion, which cannot be modeled in a simple way and will require a more detailed investigation. Besides providing a general model for the diffusion in an interacting noisy system, this study highlights the capability of quantum gases in disordered optical potentials to investigate other general problems related to noise in quantum systems.

2. Experimental setup

2.1. Dynamics in a quasi-periodic lattice

The experiment is based on a Bose–Einstein condensate of ^{39}K atoms in the fundamental energy band of a quasi-periodic potential, which is generated by perturbing a strong primary optical lattice with a weak, incommensurate, secondary one (figure 1(a)). The site-to-site tunneling energy J of the main lattice and the quasi-disorder strength Δ characterize the corresponding Hamiltonian [42]. In the non-interacting case the system shows an Anderson-like localization transition for a finite value of the disorder $\Delta = 2J$. Above this threshold all eigenstates are exponentially localized, with a localization length $\xi \approx d/\ln(\Delta/2J)$ [43], where d is the spacing of the main lattice.

The noise is introduced by an amplitude modulation of the secondary lattice, with controllable strength A and with frequency ω_m that is randomly varied in a proper interval (see appendix A). This corresponds to a broadband spectrum with a controllable width of the same order as the energy bandwidth of the quasi-periodic potential, i.e. $W \approx 2\Delta + 4J$. We note that our noise is non-dissipative, and in general, we have an out-of-equilibrium situation in which the fluctuation–dissipation relation does not hold. However, the finite bandwidth of the lattice sets a limit of the order of $4J$ to the maximum kinetic energy that can be pumped into the system by the noise source. Numerical simulations we performed indicate that after a typical time $t = 0.1\text{--}1$ s our system has reached this limit, and most of the long-time dynamics happens in a quasi-equilibrium regime.

A magnetic Feshbach resonance allows one to control the contact interaction [44], by tuning the s-wave scattering length a and in turn the mean interaction energy per particle $E_{\text{int}} \approx 2\pi\hbar^2 a\bar{n}/m$, where \bar{n} is the mean density and m is the particle mass.

To study the dynamics, we initially prepare the condensate close to the ground state of the lattice, also in presence of a tight axial trap. We then switch off the trap and study the expansion dynamics along the lattice, thanks to an additional radial confinement. To do so, we detect the

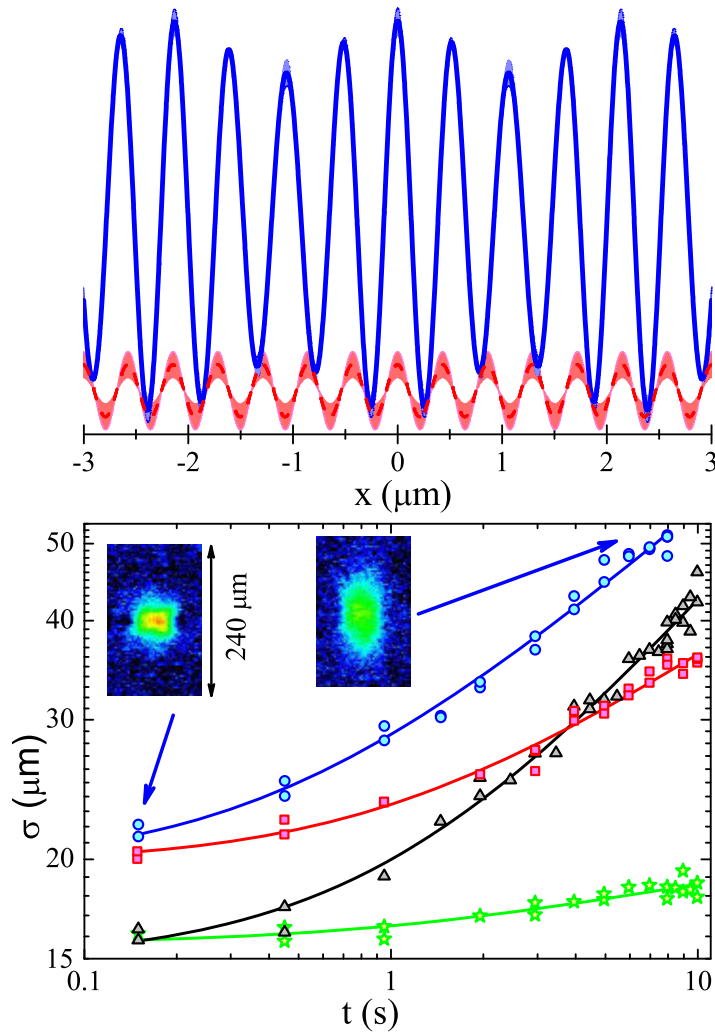


Figure 1. Expansion with disorder, noise and interaction. (a) Noisy quasi-periodic potential (solid line), realized by a static main optical lattice overlapping a secondary one (dashed line), with a broadband amplitude modulation. (b) Measured time evolution of the width for different values of noise amplitude and interaction energy for $\Delta/J = 4$: $A = 0$ and $E_{\text{int}} \sim 0$ (stars), $A = 0.9$ and $E_{\text{int}} \sim 0$ (triangles), $A = 0$ and $E_{\text{int}} \sim 0.8J$ (squares) and $A = 0.8$ and $E_{\text{int}} \sim 0.8J$ (circles). The lines are fits to equation (2).

axial density profile $n(x, t)$ with destructive absorption imaging at increasing times t , up to $t = 10$ s. The measurements we present are typically referred to as the root mean square (rms) width σ of the sample along the lattice.

3. Results

3.1. Observation of anomalous diffusion induced by noise and interaction

A typical time evolution of the width of the system for $\Delta > 2J$ in the presence of noise and interaction is shown in figure 1. The disorder-induced localization is broken by interaction

or noise alone and also by their combination. In all cases, we observe a short-time transient that evolves into asymptotic behavior, which is different in the three cases. To analyze the expansion, we start by recalling that a solution of the diffusion equation

$$\frac{\partial n(x, t)}{\partial t} = \frac{1}{2} \frac{\partial}{\partial x} \left(D \frac{\partial n(x, t)}{\partial x} \right) \quad (1)$$

is a Gaussian distribution $n(x, t) \approx \exp[-x^2/2\sigma(t)^2]$, with $d\sigma^2(t)/dt = D$. This would imply a time dependence of the distribution width as

$$\sigma(t) = \sigma_0(1 + t/t_0)^\alpha \quad (2)$$

with the time exponent $\alpha = 0.5$. For our experimental distributions, we find that a solution of a generalized diffusion equation of the form of equation (2) with α as a free parameter can be used to fit the rms width of $n(x, t)$ in all cases. Here σ_0 is the initial width, t_0 is a free parameter that represents the crossover time from the short-time dynamics to the asymptotic regime and the exponent α characterizes the expansion at long times. In our data, we typically see about one decade (in time) of asymptotic expansion. In the presence of noise alone we typically observe normal diffusion, i.e. $\alpha = 0.5$, as expected in the case of white noise. The dynamics is instead sub-diffusive, i.e. $\alpha < 0.5$, in the presence of a repulsive interaction; as we will discuss later, this is essentially due to a reduction of the interaction coupling as the system expands. In the presence of both noise and interaction, we typically observe a non-trivial anomalous diffusion, with expansion exponent α depending on the relative value of interaction energy E_{int} and noise amplitude A . As we discussed above, we are not aware of any theory for this combined problem. We therefore model the expansion with a generalized diffusion equation for $\sigma^2(t)$ where the instantaneous diffusion coefficient is the sum of the two coefficients of interaction and noise alone, i.e.

$$\frac{d\sigma^2(t)}{dt} = D_{\text{noise}} + D_{\text{int}}(t). \quad (3)$$

Here $D_{\text{noise}} = \text{const}$ is the diffusion coefficient due to noise alone, whereas $D_{\text{int}}(t)$ is the time-dependent diffusion coefficient for interaction alone. A main result of this work is that such a general diffusion equation is valid in a wide range of parameters, as we will show in detail in the following through an analysis of the individual diffusion mechanisms and their combination. A similar generalized diffusion equation has been theoretically predicted for Brownian motion of classical interacting particles [45].

3.2. Noise-induced normal diffusion

Let us start by exploring in detail the effect of noise on the dynamics of the linear system, which we realize by tuning the scattering length a close to zero. As shown in figure 1(b), we observe that a finite noise amplitude $A \neq 0$ results in a slow expansion of the initially localized sample. The shape of $n(x)$ keeps being Gaussian at all times. We fit $\sigma(t)$ to equation (2); from these and other data we measure $\alpha = 0.45(5)$, which is therefore consistent with normal diffusion, and we extract a diffusion coefficient $D = \sigma_0^2/t_0$.

We have performed an extensive investigation of the diffusion dynamics, by exploring different values of the noise amplitude A and the disorder strength Δ/J , i.e. different localization lengths. The measured diffusion coefficients D , shown in figure 2, are in good agreement with numerical simulations in terms of a generalized Aubry–André model [30, 46], including a dynamical disorder analogous to the experimental one (appendix B).

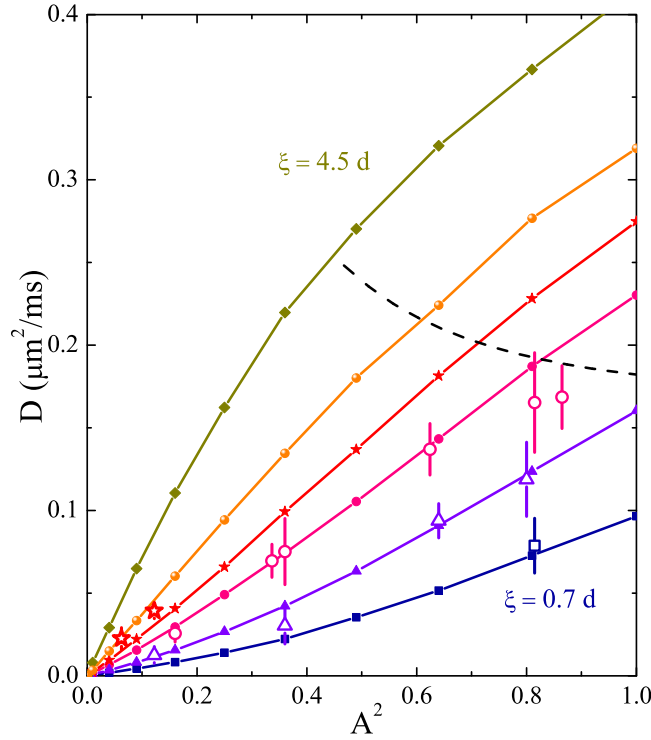


Figure 2. Noise-induced normal diffusion: ξ and A dependence of the diffusion coefficients. (a) Measured diffusion coefficient D versus the square of the noise amplitude A , for different values of the disorder strength. From top to bottom: $\Delta/J = 2.5$ (rhombuses), 3 (spheres), 3.5 (stars), 4 (circles), 5.5 (triangles) and 8 (squares). The open symbols stand for the experimental measurements and the filled ones for numerical simulations. The dashed line represents the critical values of the noise strength A_c and D above which the perturbative approach is no longer valid (see appendix B).

We can interpret the observed diffusion as incoherent hopping between localized states driven by the broadband noise. A perturbative approach suggests that $D \propto \Gamma \xi^2$ and $\Gamma \propto A^2$, where the localization length ξ represents the natural length scale of the hopping and Γ is the perturbative transition rate [19]. For the Aubry–André model, in the limit of a noise bandwidth equal to the lattice bandwidth, we calculate a diffusion coefficient

$$D \propto \frac{A^2 J (\xi + d)^2}{\hbar (1 + e^{d/\xi})}, \quad (4)$$

which is in good agreement with both the experiment and numerical simulations (appendix B). As shown in figure 2, we observe the linear dependence of D on A^2 and also an increase of D with ξ .

The described behavior persists in most of the range of values of A and ξ we have been able to explore in the experiment. The simulations, however, give a clear indication that large values of A and/or ξ would bring the system into a different regime, where the dependence on the localization length becomes weaker. This is expected since, in the presence of sufficiently strong noise, the perturbative approach based on localized states must fail. Interestingly, the

experimental data, the numerical ones and the perturbative model indicate that the crossover to this second regime happens at strong noise amplitudes, $A \approx 1$, for our range of rather short localization lengths, i.e. $\xi \approx d$.

3.3. Interaction-induced subdiffusion

We now discuss the effect of the interaction, which is introduced in our system by changing the scattering length a to a finite value, hence introducing a finite E_{int} . The effect of such nonlinearity on the dynamics on a lattice with static disorder has already been studied in theory [26–32] and experiments [25, 37]. Basically, the finite interaction energy breaks the orthogonality of the single-particle localized states, weakening the localization. In this case one can describe perturbatively the resulting dynamics as an interaction-assisted coherent hopping between localized states, with a coupling strength that decreases as the sample expands, since the density and hence E_{int} decrease [37]. This results in subdiffusive behavior, i.e. in diffusion with a decreasing instantaneous diffusion coefficient

$$D_{\text{int}}(t) = 2\alpha_{\text{int}} \frac{\sigma_0^{\alpha_{\text{int}}^{-1}}}{t_0} \sigma(t)^{2-\alpha_{\text{int}}^{-1}}, \quad (5)$$

where α_{int} is the time exponent. From $d\sigma(t)^2/dt = D_{\text{int}}(t)$, one gets indeed an evolution of the form $\sigma(t) = \sigma_0(1+t/t_0)^{\alpha_{\text{int}}}$. The precise value of such an exponent depends on the details of the interaction strength and of the spatial correlations of the disorder: for an uncorrelated random disorder and $E_{\text{int}} \approx \Delta$, a perturbative approach predicts $\alpha_{\text{int}} = 0.25$. In our experiment, we find exponents in the range $0.2 < \alpha_{\text{int}} < 0.35$. A detailed description of the various regimes achievable in a quasi-periodic lattice can be found in [47].

3.4. The generalized diffusion model

When we introduce noise and interaction at the same time, we observe an expansion that is globally faster than that for noise or interaction alone. Note that the solution of equation (3) will result in a time-dependent exponent $\alpha(t)$ such that equation (2) does not hold anymore. However, given the experimentally limited time window, it is still possible to fit well the observed behavior by (2) with a transient exponent $0.3 < \alpha' < 0.5$, which is intermediate between the two previous ones. This indicates that both delocalization mechanisms are playing a role in the expansion. One example over many of these observations is shown in figure 3, which reports three characteristic expansion curves for noise or interaction alone, or both. In the presence of both noise and interaction, we also find that the distribution does not manifestly deviate from a Gaussian during the expansion. To analyze the combined dynamics, we use the generalized diffusion equation (3), where D_{noise} and $D_{\text{int}}(t)$ are separately extracted by fitting, respectively, the case with noise alone and interaction alone to equation (2). The numerical solution of the differential equation (3) is actually in good agreement with the experimental data and also with the numerical results of the theoretical model, as shown in figure 3.

These examples of the experimental observations and numerical simulations strongly support the hypothesis of additivity of the two delocalization mechanisms, at least at first order. In the experimental data (see figures 3(a) and (b)), we typically observe a slightly faster diffusion with noise and interaction. This difference is due to the axial excitation in the presence of noise, which in turn excites the radial degrees of freedom in the presence of interaction [37]

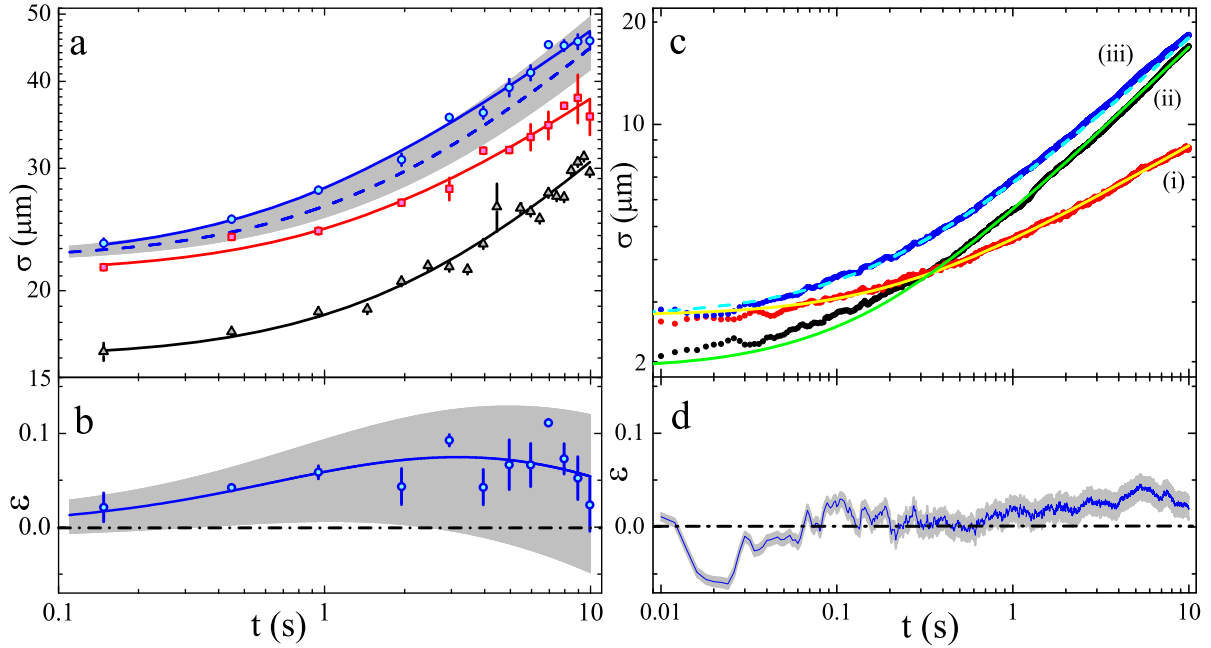


Figure 3. Noise and interaction additive anomalous diffusion. (a) Measured time evolution of the width for noise alone (triangles), interaction alone (squares) or both (circles) for $\Delta/J = 4$. The noise amplitude is $A = 0.6$, while the interaction strength is $E_{\text{int}} \sim 0.8J$. The experimental data are fitted to equation (2) (solid lines). The dashed line is the numerical solution of equation (3) using the extracted diffusion coefficients from the fits, with the confidence interval shown as a gray area. (b) Relative residuals of the fit, for the case with noise and interaction, and the solution of equation (3), with the associated confidence interval (gray area). (c) Numerical simulation of the time evolution of the width for interaction alone (i), noise alone (ii) and both (iii) for $\Delta/J = 2.5$, $J = 180$ Hz, $A = 0.195$, $T = 1$ ms and $E_{\text{int}} = 1.6J$. The numerical data are fitted to equation (2) (solid lines), whereas the dashed line is the numerical solution of equation (3). (d) Relative residuals of the numerical $\sigma(t)$ with noise and interaction (iii) and the solution of equation (3). The gray area represents the confidence level of two standard deviations.

and produces the increased expansion we observe in figure 3(b). In contrast, in numerical simulations, which neglect the axial-to-radial coupling, there are much smaller deviations from the solution of equation (3), of the order of a few lattice constants (see figure 3(d)).

The good agreement between the experimental data and the prediction of equation (3) persists for the whole range of A and E_{int} that are accessible in the experiment, with A ranging from 0.4 to 1 and E_{int} adjustable up to $\approx J$. Furthermore, as we described above (figure 2), in numerical simulations we can explore the region of large A and/or ξ , where the perturbative description of the noise effect fails. Interestingly enough, although this regime is not perturbative, we find the additivity of noise and interaction mechanisms also in this case.

An investigation over a broad range of parameters in theory indicates that the system should behave in a fully symmetric way for attractive and repulsive interactions, provided that also

the energy distribution is reversed when changing the sign of the interaction. For example, the diffusion dynamics for a repulsive system initially prepared in a potential minimum is equivalent to that of an attractive system initially prepared in a potential maximum. We have experimentally tested this expectation with a sample prepared with attractive interaction ($a \approx -100a_0$ with a_0 being the Bohr radius), where the behavior is fully analogous to that in figures 3(a) and (b), i.e. the two sources of delocalization simply add up. Note that systems prepared with $a < 0$ do not have a stable state at low energy, but typically occupy the whole energy band in a way similar to the $a > 0$ case.

Therefore, the large region of validity of equation (3) supports the idea that the observed anomalous diffusion is driven by the additivity of the two delocalization mechanisms, which indeed act independently. Note that the interaction-assisted diffusion tends to vanish as the sample expands, so that one should expect a long-time crossover to a regime where interaction effects are negligible, and the system diffuses normally due to noise alone. While we can clearly observe this crossover in the simulations, its experimental characterization is prevented by the limited observation time.

4. Regimes of noise–interaction interplay

While all experimental observations are well described by the generalized diffusion model discussed above, our numerical simulations indicate that deviations might appear when the system is subjected to a trapping mechanism. This can happen in both cases of noise with a bandwidth $\delta\nu$ much smaller than the system one W/h or of an interaction that is strong enough to produce self-trapping [30, 32, 38]. In both cases, the simulations show an interplay of noise and interaction which cannot be described by equation (3).

In the first regime, i.e. small noise bandwidth ($\delta\nu \ll W/h$), the diffusion is much slower than for a broad noise spectrum ($\delta\nu \approx W/h$), because just a small fraction of the localized states can be coupled by the noise (see also appendix B.2). Very interestingly, the addition of the interaction in this regime seems to restore a fast expansion, as if the additional coupling mechanism between localized states provided by the interaction, increasing the number of occupied states, would effectively broaden the noise spectrum. One example of this behavior is shown in figure 4, where $\delta\nu$ is ten times smaller than that in figures 3(c) and (d). One observes a noise-induced diffusion coefficient D that is smaller than that in the case of broadband noise. Interaction is able to restore a diffusion comparable with that obtained with interaction and broadband noise and is therefore much faster than that predicted by the additivity conjecture.

Note that in this regime the additivity hypothesis fails despite the validity of our perturbative approach to describe the noise-induced diffusion. This example and the complementary case of a strong noise which manifests additivity to the interaction, although the perturbative model is not valid, indicate the independence of the additivity conjecture from the validity of the perturbative description of the noise.

The second regime, i.e. self-trapping, is a general scenario for the expansion in lattices in the presence of interaction, which is reached when E_{int} is too large to be transformed into kinetic energy during the expansion [30, 38], and the bulk of the system is effectively localized. An example is shown in figure 5, where the self-trapping is achieved by introducing an attractive interaction on an initial state that is close to the single-particle ground state of the system. Here, we observe an interplay of noise and interaction resulting in a breakdown of the additivity

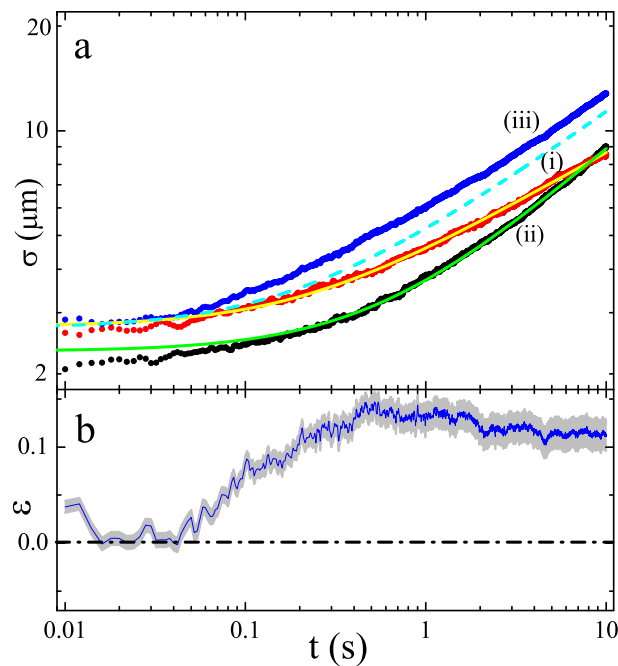


Figure 4. Deviations from additivity with a narrowband noise. Numerical simulation of the time evolution of the width (a) and relative residuals (b) with the same parameters as those of figures 3(c) and (d), but with $T = 10$ ms. Deviations from additivity are evident in the discrepancy between the curve with noise and interaction (iii) and the solution of equation (3) (dashed line).

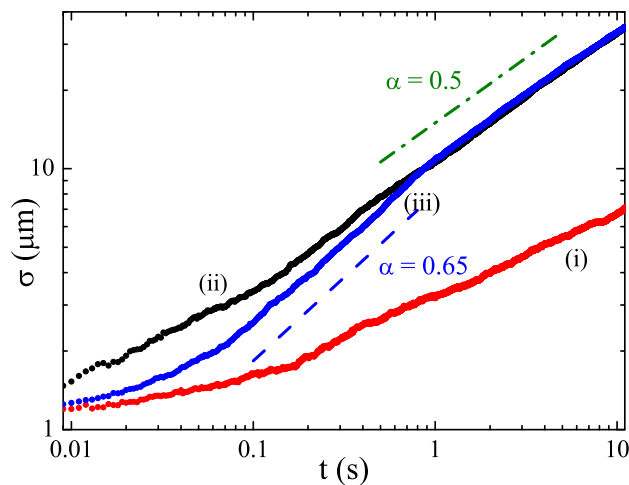


Figure 5. Deviations from additivity in the self-trapping regime. Numerical simulations of the time evolution of the width for attractive interaction alone (i), noise alone (ii) or both (iii) for $\Delta/J = 2.5$, $J = 180$ Hz, $A = 0.4$, $\beta = -35$, $T = 0.6$ ms. An intermediate super-diffusive ($\alpha > 0.5$) regime seems to be induced by self-trapping, while asymptotically one has normal diffusion with exponent $\alpha \sim 0.5$. The (green) dashed-dotted line shows the diffusive slope, while the superdiffusive one is represented by the (blue) dashed line.

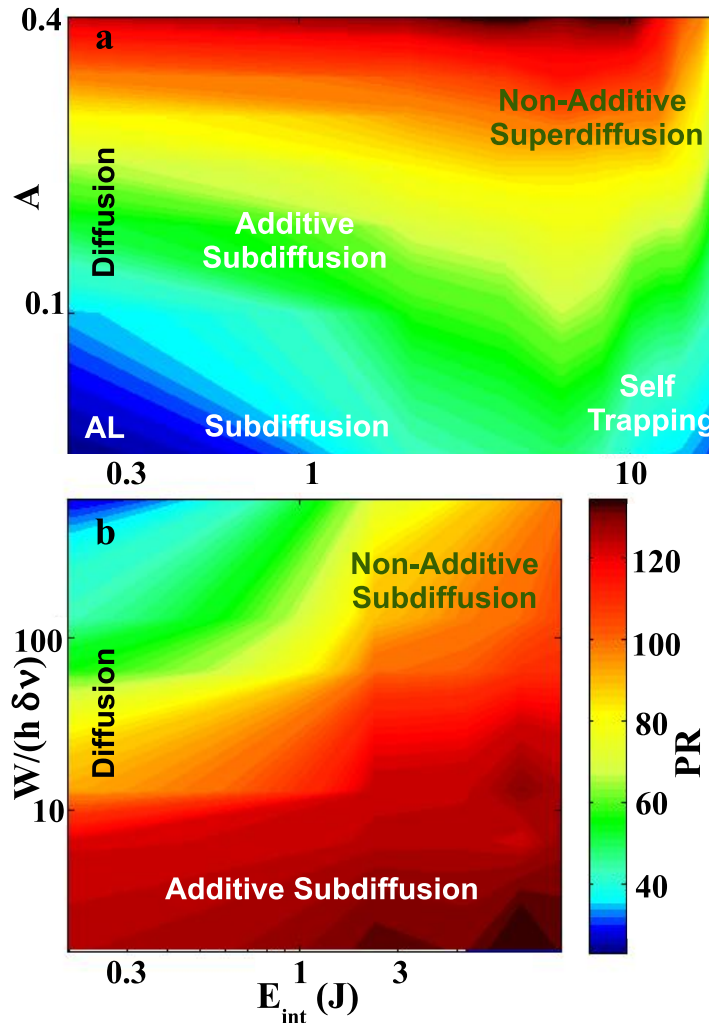


Figure 6. Generalized diffusion regimes. The color scale represents the number of significantly occupied sites after 10 s of our numerically simulated expansion, for $\Delta = 2.5J$, $J = 180$ Hz and a Gaussian wavepacket initially distributed over ≈ 13 lattice sites. (a) Dependence on A and E_{int} for a broadband noise ($\delta \nu \approx W/h$). (b) Dependence on E_{int} and $\delta \nu$, for a fixed noise strength $A = 0.4$.

and in transient superdiffusive behavior, i.e. an expansion with $\alpha > 0.5$. In the absence of noise, the central part of the distribution, where E_{int} is large, cannot expand, and therefore the rms width σ increases more slowly than normal. Noise can break this trapping by providing the necessary energy to couple the interaction-shifted states to the lattice band. This causes the fast expansion at short times, which is even faster than normal diffusion. We note that related superdiffusion effects have been predicted in linear systems with different energies [48]. An analogous effect might arise when the noise is able to release the large kinetic energy associated with the self-trapped part of the system, but further studies are needed to clarify this mechanism.

5. Summary

An effective overview of our extensive investigation can be achieved by studying the general behavior of the expansion for different A , E_{int} and δv values in numerical simulations. The quantity that is convenient to study is the so-called participation ratio, $\text{PR} = (\sum_i n_i^2)^{-1}$ (see appendix B for the details), which measures the number of significantly occupied lattice sites. The specific diagram in figure 6, which shows the calculated PR after 10s of expansion for a particular Gaussian initial distribution, can be used to summarize the general properties investigated with our system.

For broadband noise (figure 6(a), $\delta v \approx W/h$), one finds again that Anderson localization is suppressed by either noise or interaction, with both leading to an expansion of the system. We remark that the mechanisms underlying these two expansions are quite different. A weak interaction produces a coherent coupling of single-particle localized states; the resulting transport can be modeled as a coherent hopping between such states, with characteristic subdiffusive behavior that is determined by the changing density. Noise instead drives an incoherent hopping between localized states, which results in a diffusive expansion. Once both transport mechanisms are combined, one sees an enhanced expansion, as highlighted by the increasing width in figure 6(a) for finite A and E_{int} . Our detailed time-dependent analysis indicates that this combined diffusion is well modeled by the generalized, additive diffusion model of equation (3). This surprisingly simple result seems to be not limited to the region of parameters where the noise- or interaction-induced diffusions can be modeled perturbatively.

The numerical simulations reveal also a region of stronger interaction ($E_{\text{int}} \approx 4J$), where the interaction itself prevents expansion, because of the self-trapping mechanism. This is visible as a reduction of the PR for increasing E_{int} in figure 6(a). Here, the addition of noise restores a diffusion, which our time-dependent analysis has shown to have an anomalous superdiffusive nature. In this regime, the model of equation (3) clearly breaks down.

Finally, an interplay of noise and interaction is seen also in the presence of narrowband noise, as shown in figure 6(b). Here the expansion is studied for different inverse noise bandwidths, $W/h\delta v$ and E_{int} and for a fixed value of the noise strength ($A = 0.4$). In the non-interacting regime, the diffusion constant decreases with increasing $W/h\delta v$. On the addition of the interaction a faster expansion is recovered, which, however, cannot be described by equation (3).

6. Conclusions and outlook

In conclusion, we have experimentally realized an ultra-cold atomic system to investigate the transport of a wavepacket in the presence of controllable disorder, noise and interaction. We have used it to characterize the noise-induced diffusion and its interplay with an interaction-induced subdiffusion. We have observed that the complex anomalous diffusion resulting from the simultaneous presence of the two processes can be remarkably explained by a simple generalized diffusion equation in a wide range of parameters. Finally, we have numerically observed also regimes where the presence of trapping phenomena produces a more complex interplay between the noise- and interaction-induced diffusion mechanisms. It is interesting to note that a quasi-periodic lattice might allow one to study also a different regime that has been extensively analyzed in theory [16, 49, 50], in which in the absence of noise all the eigenstates are extended, while the noisy potential is disordered. This regime can be achieved simply by

using a weaker disorder, below the localization threshold ($\Delta < 2J$). Preliminary numerical simulations we have performed show that in this case the noise slows the dynamics from ballistic to diffusive.

Our work has shown how the combination of an ultra-cold atomic system with optical lattices can be effectively employed to study quantum phenomena related to noise. Future experiments in lattices with higher dimensionality or in reduced dimensions will allow one to explore the regime of strong correlations. Here there is strong interest in understanding the behavior of open quantum systems [51], and how quantum phase transitions are affected by noise [52]. An interesting alternative to the use of a noisy optical potential is to employ a large sample of a second atomic species with a controllable thermal distribution, which is coupled via resonant elastic scattering to the atomic system under study. This approach might allow one to introduce a noise in thermal equilibrium, and to simulate phonon-related phenomena [53, 54].

Furthermore, our scheme could be easily used to control the temperature of our weakly interacting bosons in the presence of disorder in order to investigate the many-body metal–insulator transitions at finite temperatures [55].

Acknowledgments

We thank Lorenzo Gori for valuable contributions to the experiment and Shmuel Fishman and Michele Modugno for fruitful discussions. This work was supported by the ERC projects QUPOL and DISQUA, the EU projects Q-ESSENCE and AQUATE, the EU Marie-Curie Programme, MIUR (FIRB-RBFR10M3SB and PRIN-2009FBKLNN) and the Alexander von Humboldt Foundation. BD acknowledges support from the Carl-Zeiss-Stiftung. The QSTAR is the MPQ, LENS, IIT, UniFi Joint Center for Quantum Science and Technology in Arcetri. FC acknowledges QSTAR as well as the Imperial College High Performance Computing Service for computational resources.

Appendix A. Experimental methods

A.1. Quasi-periodic potential

The one-dimensional quasi-periodic potential is created by a primary optical lattice combined with a weaker incommensurate one:

$$V(x) = V_1 \sin^2(k_1 x + \varphi_1) + V_2 \gamma^2 \sin^2(\gamma k_1 x + \varphi_2). \quad (\text{A.1})$$

Here $k_i = 2/\lambda_i$ are the wavevectors of the lattices ($\lambda_1 = 1064.4$ nm and $\lambda_2 = 859.6$ nm) and $\gamma = \frac{\lambda_1}{\lambda_2}$ measures the commensurability of the lattices. The relevant parameters are the spacing $d = \lambda_1/2$, the tunneling energy J (typically 150 Hz) of the primary lattice and the disorder strength Δ , which scales linearly with V_2 [46]. Non-interacting particles in the fundamental band of this lattice are described by the Aubry–André model [43] which shows a metal–insulator transition for a finite value of the disorder $\Delta = 2J$ [46].

A.2. Interaction energy

The scattering length a is changed by means of a broad Feshbach resonance to values ranging from $a \approx 0.1a_0$ to about $a = 300a_0$ [44]. We can define a mean interaction energy per atom $E_{\text{int}} = 2\pi\hbar^2 a \bar{n}/m$, where \bar{n} is the mean on-site density. The atomic sample is radially trapped

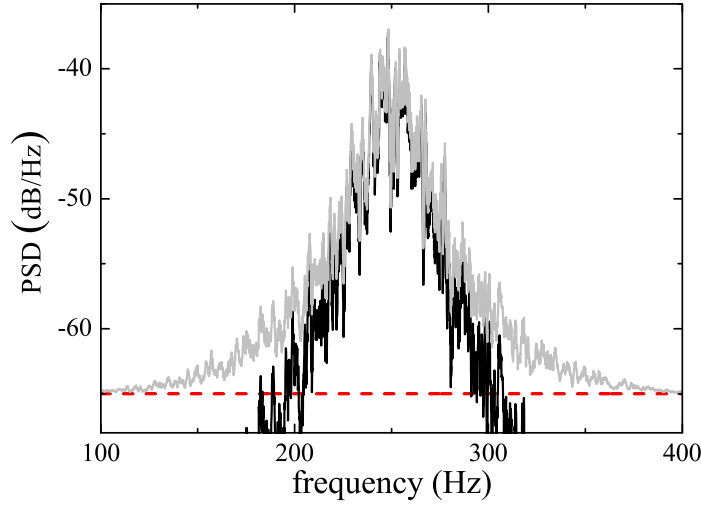


Figure A.1. Noise spectrum. Typical noise spectral density for $T = 5$ ms and $A = 1$ (black-solid line). By including the broadband background noise (red dashed line), due to acoustic noise on the lattices' mirrors, we estimate the effective experimental spectrum (gray solid line).

with a frequency $\omega_r = 2\pi \times 50$ Hz. The presence of the radial degrees of freedom limits E_{int} to values that are not much larger than the kinetic energy J or the disorder energy Δ .

A.3. Noise implementation

In order to have a controllable amount of noise, we introduce a time dependence on the amplitude of the secondary lattice potential, which produces a time variation of the on-site energies. In the experiment, the noise must be broadband enough to couple to as many states as possible within the lattice bandwidth ($W/\hbar \approx (2\Delta + 4J)/\hbar$), but at the same time one must avoid excitation of the radial modes ($\omega_r = 2\pi \times 50$ Hz) as well of the second band of the lattice ($\Delta E_{\text{gap}}/h \approx 3\text{--}5$ kHz). This is achieved with a sinusoidal amplitude modulation, i.e.

$$V_2(t) = V_0(1 + A \sin(\omega_m t + \phi_m)) \quad (\text{A.2})$$

with the frequency ω_m that is randomly varied in a finite interval $\omega_m \in [\omega_0 - \delta\omega, \omega_0 + \delta\omega]$ with a time step T , while the phase ϕ_m is adjusted to preserve the continuity of the modulation and the sign of its first derivative and to avoid frequency components outside the chosen band. The values used in the experiment, whose typical spectrum is shown in figure A.1, are $\omega_0/2\pi = 250$ Hz, $\delta\omega_0/2\pi = 50$ Hz and $T = 5$ ms. At long times, $t \gg T$ the resulting noise spectrum decays exponentially outside the band $[\omega_0 - \delta\omega, \omega_0 + \delta\omega]$, on a frequency scale $\approx 1/T$. Note that at short times, $t \approx T$, this spectrum contains only a few components, which might result in an inefficient excitation of the localized states to provide diffusion [56]. In the experiment, however, we do not see such an effect. We believe that this is due to an additional broadband background noise in the relative phase of the two lattices, which is due to fluctuations of the position of the retroreflecting mirror at acoustic frequencies. We measured this phase noise via a Michelson interferometer scheme, and we estimate it to be equivalent to a broadband amplitude noise on the secondary lattice, about 25 dB below the main noise when $A = 1$. The estimated value is consistent with the small diffusion we have for $A = 0$ and with the diffusion we observe for $A > 0$ and a single frequency modulation, i.e. $\delta\omega = 0$.

In the numerical simulations, we find, however, a reduced expansion until $t \gg T$. For this reason, we have numerically tested also a second noise scheme corresponding to a larger width of the power spectrum already at short times and is able to better reproduce the experimental combination of the external frequency noise and the uncontrollable phase one. In this scheme the frequency ω_m is kept fixed, while the phase ϕ_m is randomly varied every time step T . Here, the power spectrum is essentially a sinc function with width $\delta\omega = 2\pi/T$ as soon as $t > T$.

We have checked with extensive simulations that both types of noise lead to normal diffusion at long times. In the second case, we observe that the diffusion coefficient D grows linearly with the bandwidth of the noise as long as such a bandwidth is smaller than the lattice bandwidth W/\hbar . Larger bandwidths, i.e. very small T , actually lead to a reduction of D , since not all the frequencies can effectively produce hopping between the localized states.

Appendix B. Theoretical methods

B.1. The theoretical model

The numerical simulations presented in the paper are based on a generalized version of the Aubry–André model [43], including a mean-field interaction term [30, 46]:

$$i\dot{\psi}_j(t) = -(\psi_{j+1}(t) + \psi_{j-1}(t)) + V_j|\psi_j(t)|^2 + \beta|\psi_j|^2\psi_j, \quad (\text{B.1})$$

where $V_j = \Delta/J \sin(2\pi\gamma j)$, β is the interaction strength and $\psi_j(t)$ are the coefficients of the wave function in the Wannier basis, normalized in such a way that their squared modulus corresponds to the atom density on the j th site of the lattice. All energies are measured in units of the next-neighbor tunneling energy J , while the natural units for time are \hbar/J . Note that this model can describe only the lowest energy band of the real system. Excited bands are, however, not populated in the experiment. The interaction parameter β in the model can be connected to the mean interaction energy per particle in the real system, which is defined as

$$E_{\text{int}} = \frac{2\pi\hbar^2}{m} a \frac{\int n(\mathbf{r})^2 d^3r}{\int n(\mathbf{r}) d^3r}. \quad (\text{B.2})$$

Here $n(\mathbf{r})$ is the mean on-site density distribution, i.e. the solution of the interacting Gross–Pitaevskii problem in a single well, normalized to an atom number N/\bar{n}_s , where \bar{n}_s is the mean number of sites occupied by the atomic distribution. The relation between E_{int} and the interaction strength in the model is approximately $E_{\text{int}} \approx 2J\beta/\bar{n}_s$ [30, 46].

To quantify the localization, we consider two quantities: the width of the wavepacket measured as the square root of the second moment of the spatial distribution $|\psi_j(t)|^2$,

$$\sigma(t) = \sqrt{m_2(t)} = \left[\sum_j (j - \langle j \rangle)^2 |\psi_j(t)|^2 \right]^{1/2} \quad (\text{B.3})$$

and the participation ratio PR,

$$\text{PR}(t) = \frac{1}{\sum_j |\psi_j(t)|^4} \quad (\text{B.4})$$

measuring the number of significantly occupied lattice sites. The quantity $\langle j \rangle$ represents the average over the spatial distribution, defined as $\langle j \rangle = \sum_j j |\psi_j|^2$.

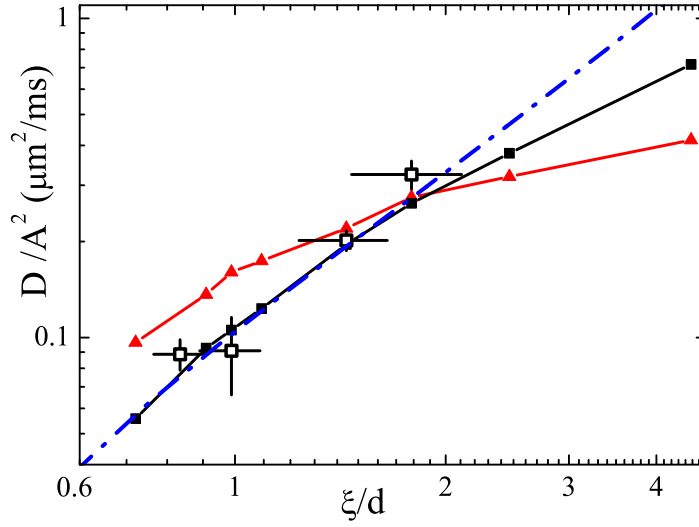


Figure B.1. Noise-induced normal diffusion: the ξ dependence of the diffusion coefficients. Normalized diffusion coefficient D/A^2 versus the localization length ξ for the regime of small noise strength A in both experiment (open squares) and numerical simulations (filled squares) and for $A = 1$ in simulations (triangles). The dash-dotted line shows the prediction with the perturbative approach. For numerical data, solid lines are just a guide to the eyes.

B.2. Perturbative approach to noise-induced diffusion

In this section, we consider a perturbative approach to describe the diffusion induced by noise. The dynamics of the disordered system in the absence of temporal noise is described by equation (B.1). In the regime of small noise amplitude ($A \ll 1$), we can assume that the only effect of noise is to induce hopping between different localized states of the unperturbed system. The coupling is driven by the frequency component of the noise spectrum that is resonant with the energy difference between the states. In the regime of $\xi \approx d$ investigated in this work, we can restrict our analysis just to the coupling between neighboring states. The hopping rate depends on the noise strength and on the overlap between the noise spectrum $s(\nu)$ and the unperturbed system energy distribution $P(\nu)$:

$$\Gamma = \frac{A^2 J}{\hbar} \eta \left(\frac{\Delta}{J} \right)^2 |\langle i | \sin(2\pi \gamma j) | f \rangle|^2, \quad (\text{B.5})$$

where $\eta = \frac{1}{A^2} \int s(\nu) P(\nu) d\nu$ is $\lesssim 1$. To obtain an analytic prediction of the effect of the noise, we approximate the energy difference between states as a flat spectrum with the same width as the lattice band, $W/h \approx (2\Delta + 4J)/h$. We approximate the overlap $|\langle i | \sin(2\pi \gamma j) | f \rangle|^2$ with $|\langle i | f \rangle|^2$, where the states $|i\rangle$ and $|f\rangle$ are assumed to be exponentially localized over a distance ξ . It is also reasonable to consider $\Delta/J \sim 2e^{d/\xi}$. Finally, when the noise spectrum is a sinc function with T equal to the inverse of the bandwidth W/h , we obtain an analytical estimation of the diffusion coefficient

$$D = \xi^2 \Gamma \approx \frac{A^2 J}{3\hbar} \frac{(\xi + d)^2}{1 + e^{d/\xi}}. \quad (\text{B.6})$$

This expression is evaluated for the optimal case of $T = h/W$, which determines the specific numerical prefactor $1/3$. In the general case, we find a more complex dependence of D on ξ , and a coefficient D that decreases with the width of the noise spectrum $\delta\nu = 1/T$, i.e. the overlap between $s(\nu)$ and $P(\nu)$ decreases. As shown in figure B.1, the diffusion coefficient obtained with this heuristic model almost perfectly captures the evolution of D with both A and ξ . Nevertheless, we numerically observe that the perturbative approach does not hold for large values of A and ξ , i.e. $\xi \geq 2d$. In these regimes, in fact, the ξ dependence of D becomes weaker. The good agreement between the perturbative model and the observed evolution of D confirms the picture that this diffusion is induced by the hopping between localized states, in analogy with other disordered noisy systems, such as the kicked rotor with noise [18].

We can estimate that the perturbative approach fails when the energy associated with the perturbation rate becomes comparable with the mean separation energy between states in a localization volume, i.e. $\hbar\Gamma \approx \Delta \frac{d}{3\xi}$. This corresponds to a critical noise amplitude

$$A_c \approx \left(2 e^{d/\xi} \frac{1 + e^{d/\xi}}{\left(1 + \frac{d}{\xi}\right)^2} \frac{d}{3\xi} \right)^{1/2}. \quad (\text{B.7})$$

As shown in figure 2, A_c and the relative D , calculated using respectively equations (B.6) and (B.7), correctly capture the order of magnitude for the transition from the perturbative regime into a new regime in which the ξ dependence of D is weaker. On top of this, the fact that A_c increases as ξ decreases, i.e. when the disorder is stronger, is also reproduced by our simulations.

There is a further regime of strong disorder that can, in principle, be conceived in which the localization length is smaller than the lattice spacing and d becomes therefore the relevant length scale for the diffusion [18]. This has so far not been accessible in the experiment, because the resulting diffusion is too slow to be characterized accurately.

References

- [1] Kramer B and MacKinnon A 1993 *Rep. Prog. Phys.* **56** 1469
- [2] Bouchard J-P and Dean D S 1995 *J. Physique I* **5** 265–86
- [3] Hänggi P and Marchesoni F 2009 *Rev. Mod. Phys.* **81** 387–442
- [4] Plenio M B, Hartley J and Eisert J 2004 *New J. Phys.* **6** 36
- [5] Caruso F, Huelga F and Plenio M B 2010 *Phys. Rev. Lett.* **105** 190501
- [6] Mohseni M, Rebentrost P, Lloyd S and Aspuru-Guzik A 2008 *J. Chem. Phys.* **129** 174106
- [7] Plenio M B and Huelga S 2008 *New J. Phys.* **10** 113019
- [8] Olaya-Castro A, Lee C F, Fassioli Olsen F and Johnson F N 2008 *Phys. Rev. B* **78** 085115
- [9] Caruso F, Chin A W, Datta A, Huelga S F and Plenio M B 2010 *Phys. Rev. A* **81** 062346
- [10] Caruso F, Chin A W, Datta A, Huelga S F and Plenio M B 2009 *J. Chem. Phys.* **131** 105106
- [11] Broome M A, Fedrizzi A, Lanyon B P, Kassa I, Aspuru-Guzik A and White A G 2010 *Phys. Rev. Lett.* **104** 153602
- [12] Schreiber A, Cassemiro K N, Potocek V, Gábris A, Mosley P J, Andersson E, Jex I and Silberhorn Ch 2010 *Phys. Rev. Lett.* **104** 050502
- [13] Schreiber A, Gábris A, Rohde P P, Laiho K, Štefanák M, Potocek V, Hamilton C, Jex I and Silberhorn Ch 2012 *Science* **336** 55
- [14] Krivolapov Y, Levi L, Fishman S, Segev M and Wilkinson M 2012 *New J. Phys.* **14** 043047
- [15] Bouchard J P and Georges A 1990 *Phys. Rep.* **195** 127–293
- [16] Ovchinnikov A A and Erikhman N S 1975 *J. Exp. Theor. Phys.* **40** 733

- [17] Madhukar A and Post W 1977 *Phys. Rev. Lett.* **39** 1424
- [18] Ott E, Antonsen T M and Hanson J D 1984 *Phys. Rev. Lett.* **53** 2187
- [19] Fishman S and Shepelyansky D L 1991 *Europhys. Lett.* **16** 643–8
- [20] Cohen D 1991 *Phys. Rev. Lett.* **67** 1945
- [21] Bayfield J E 1991 *Chaos* **1** 110
- [22] Blümel R, Graham R, Sirko L, Smilansky U, Walther H and Yamada K 1989 *Phys. Rev. Lett.* **62** 341
- [23] Arndt M, Buchleitner A, Mantegna R N and Walther H 1991 *Phys. Rev. Lett.* **67** 2435
- [24] Steck D A, Milner V, Oskay W H and Raizen M G 2000 *Phys. Rev. E* **62** 3461
- [25] Lahini Y, Avidan A, Pozzi F, Sorel M, Morandotti R, Christodoulides D N and Silberberg Y 2008 *Phys. Rev. Lett.* **100** 013906
- [26] Shepelyansky D L 1993 *Phys. Rev. Lett.* **70** 1787
- [27] Kopidakis G, Komineas S, Flach S and Aubry S 2008 *Phys. Rev. Lett.* **100** 084103
- [28] Pikovsky A S and Shepelyansky D L 2008 *Phys. Rev. Lett.* **100** 094101
- [29] Flach S, Krimer D O and Skokos C 2009 *Phys. Rev. Lett.* **102** 024101
- [30] Larcher M, Dalfovo F and Modugno M 2009 *Phys. Rev. A* **80** 053606
- [31] Flach S 2010 *Chem. Phys.* **375** 548–56
- [32] Kolovsky A R, Gómez E A and Korsch H J 2010 *Phys. Rev. A* **81** 025603
- [33] Wellens T and Grémaud B 2008 *Phys. Rev. Lett.* **100** 033902
- [34] Schwiete G and Finkelstein A M 2010 *Phys. Rev. Lett.* **104** 103904
- [35] Cherroret N and Wellens T 2011 *Phys. Rev. E* **84** 021114
- [36] Deissler B, Zaccanti M, Roati G, D’Errico C, Fattori M, Modugno M, Modugno G and Inguscio M 2010 *Nature Phys.* **6** 354–8
- [37] Lucioni E, Deissler B, Tanzi L, Roati G, Zaccanti M, Modugno M, Larcher M, Dalfovo F, Inguscio M and Modugno G 2011 *Phys. Rev. Lett.* **106** 230403
- [38] Smerzi A, Fantoni S, Giovanazzi S and Shenoy S R 1997 *Phys. Rev. Lett.* **79** 4950
- [39] Mott N F 1968 *Rev. Mod. Phys.* **40** 677
- [40] Giamarchi T and Schulz H J 1987 *Europhys. Lett.* **3** 1287
- [41] Fisher M P A, Grinstein G and Fisher D S 1989 *Phys. Rev. B* **40** 546
- [42] Roati G, D’Errico C, Fallani L, Fattori M, Fort C, Zaccanti M, Modugno G, Modugno M and Inguscio M 2008 *Nature* **453** 895–8
- [43] Aubry S and André G 1980 *Ann. Isr. Phys. Soc.* **3** 133
- [44] Roati G, Zaccanti M, D’Errico C, Catani J, Modugno M, Simoni A, Inguscio M and Modugno G 2007 *Phys. Rev. Lett.* **99** 010403
- [45] Aranovich G L and Donohue M D 2005 *J. Phys. Chem. B* **109** 16062
- [46] Modugno M 2009 *New J. Phys.* **11** 033023
- [47] Larcher M, Lapytyeva T V, Bodyfelt J D, Dalfovo F, Modugno M and Flach S 2012 *New J. Phys.* **14** 103036
- [48] Siegle P, Goychuk I and Hänggi P 2010 *Phys. Rev. Lett.* **105** 100602
- [49] Bouchaud J P, Toutati D and Sornette D 1992 *Phys. Rev. Lett.* **68** 1787
- [50] Saul L, Kardar M and Read N 1992 *Phys. Rev. A* **45** 8859
- [51] Diehl S, Micheli A, Kantian A, Kraus B, Buchler H P and Zoller P 2008 *Nature Phys.* **4** 878
- [52] Dalla Torre E G, Demler E, Giamarchi T and Altman E 2010 *Nature Phys.* **6** 806
- [53] Thouless D J 1974 *Phys. Rep.* **13** 93
- [54] Lewenstein M, Sanpera A, Ahufinger V, Damski B, Sen(De) A and Sen U 2007 *Adv. Phys.* **56** 243
- [55] Aleiner I L, Altshuler B L and Shlyapnikov G V 2010 *Nature Phys.* **6** 900
- [56] Yamada H and Ikeda K S 1999 *Phys. Rev. E* **59** 5214